Lyot-type flat-top fibre multiwavelength filter based on polarisation-diversity loop structure

Songhyun Jo[1], *Kyoungsoo Park*[1], *Yong Wook Lee*[1,2]

[1]*Interdisciplinary Program of Biomedical Mechanical and Electrical Engineering, Pukyong National University, Busan 608-737, Republic of Korea*
[2]*School of Electrical Engineering, Pukyong National University, Busan 608-737, Republic of Korea*
E-mail: yongwook@pknu.ac.kr

Published in Micro & Nano Letters; Received on 1st July 2014; Revised on 21st September 2014; Accepted on 30th October 2014

Proposed is a Lyot-type flat-top fibre multiwavelength filter based on a polarisation-diversity loop structure, which has flat-top and lossy flat-top passbands and multiwavelength switching capability. The proposed filter is composed of a polarisation beam splitter, two half-wave plates (HWPs) and two polarisation-maintaining fibre (PMF) loops concatenated with a 60° offset between their principal axes. One of the two PMF loops is two times longer than the other. It is able to operate in a flat-top or a lossy flat-top band mode at the selected combination of the azimuthal orientation angles of two HWPs. In particular, through the adjustment of the orientation angles of the two HWPs, its multiwavelength channels can be interleaved in each mode, which cannot be realised in a previously reported Lyot-Sagnac comb filter based on a fibre coupler. In addition to the channel interleaving capability, it provides narrower passbands compared with previous fibre multiwavelength filters with the same order. To make a quantitative comparison between the passband bandwidths of the proposed filter and other filters, both −1 and −3 dB passband bandwidths of a conventional zeroth-order, a Solc-type first-order and the proposed multiwavelength filters were considered and compared with each other.

1. Introduction: A polarisation-diversity loop structure (PDLS) that can form a Sagnac interferometer loop using a polarisation beam splitter (PBS) has been used for achieving input polarisation independence in nonlinear optical switching applications [1, 2]. This PDLS can be also employed to create multiwavelength spectra induced by polarisation interference based on birefringent elements and realise their switching in the spectral domain [3, 4]. Switchable multiwavelength spectra can be utilised for optical pulse train generation [5], high-speed wavelength routing [6], optical label switching [7], multiwavelength fibre lasers [8–10] and so forth [11–13]. The wavelength switching of filter channels, which was not realised in conventional fibre-coupler-based Sagnac birefringence filters [14], was demonstrated in PDLS-based multiwavelength filters. In particular, Solc-type PDLS-based multiwavelength filters were also reported exhibiting high-order multiwavelength spectra with flat-top passbands [15]. Although the PDLS has not yet been utilised to embody Lyot-type multiwavelength filters, a Lyot-Sagnac multiwavelength filter that showed flat-top or lossy flat-top passbands was proposed by incorporating a fibre coupler and two polarisation-maintaining fibre (PMF) loops [16]. In the Lyot-Sagnac multiwavelength filter, two PMF loops were spliced with a 2.93 rad offset between their principal axes, and one of them was two times longer than the other [16]. However, its high-order multiwavelength spectra were fixed in the wavelength position and could not be switched. Another all-fibre Lyot filter was used as a wavelength-selective filter inside the cavity of a fibre laser [17]. However, high-order spectra were not incorporated for the selection of lasing wavelengths. In addition, an all-fibre Lyot filter based on 45°-tilted fibre gratings was also reported, but its high-order transmission spectra was not investigated and analysed [18]. In this Letter, we propose a Lyot-type flat-top fibre multiwavelength filter based on the PDLS, which has flat-top passbands and the capability of switching multiwavelength channels. The proposed filter is composed of a PBS, two half-wave plates (HWPs) and two PMF loops concatenated with a 60° offset between their principal axes. One of the two PMF loops is two times longer than the other. At a specific combination of the azimuthal orientation angles of the two HWPs, flat-top and lossy flat-top transmission spectra can be obtained. In particular, multiwavelength flat-top channels can be interleaved, that is, shifted by half a period, through the control of the two HWPs, which cannot be obtained in the previous Lyot-Sagnac multiwavelength filter [16]. In comparison with previous high-order fibre multiwavelength filters, the proposed filter provides channel interleaving capability and narrower passbands. The transmittance of the proposed filter was theoretically analysed, and the theoretical prediction was verified by experiments.

2. Theoretical analysis of filter operation: Fig. 1 shows the schematic diagram of the Lyot-type flat-top fibre multiwavelength filter based on the PDLS. Input light entering the PBS, which is able to split input light into two orthogonal polarisation components or combine them into one output fibre, is decomposed into two orthogonal linearly polarised components. Linear horizontal and vertical polarisation components rotate the Sagnac loop of the PDLS in a clockwise (CW) direction and a

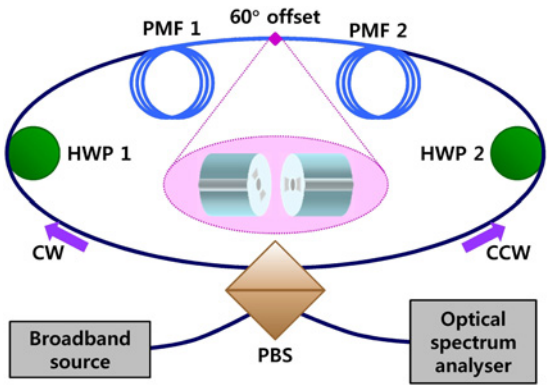

Figure 1 *Schematic diagram of the proposed filter*

doi: 10.1049/mnl.2014.0386

counterclockwise (CCW) direction, respectively. Two HWPs are placed at both ends of two concatenated PMF loops, spliced with a 60° offset between their principal axes, to control the polarisation state of light propagating through the Sagnac loop. To implement Lyot-type birefringence combination, PMF 2 was chosen to be twice as long as PMF 1 [16]. Rotating light along the CW path passes through the HWP 1, PMF 1, PMF 2 and HWP 2, and rotating light along the CCW path the HWP 2, PMF 2, PMF 1 and HWP 1 in turn. When passing through the PBS, light returning to the PBS after a roundtrip experiences linear horizontal and vertical polarisers in the CW and CCW directions, respectively.

The filter transmittance can be obtained from the mathematical analysis based on Jones formulation [19]. As shown in (1), the transfer matrix $\boldsymbol{T}$ of the proposed filter is expressed as the algebraic sum of two transfer matrices $\boldsymbol{T}_{\mathrm{CW}}$ and $\boldsymbol{T}_{\mathrm{CCW}}$. $\boldsymbol{T}_{\mathrm{CW}}$ and $\boldsymbol{T}_{\mathrm{CCW}}$ indicate the transfer matrices of the proposed filter when light rotates it along the CW and CCW paths, respectively:

$$\boldsymbol{T} = \boldsymbol{T}_{\mathrm{CW}} + \boldsymbol{T}_{\mathrm{CCW}} \tag{1}$$

$$\boldsymbol{T}_{\mathrm{CW}} = \begin{bmatrix} 1 & 0 \\ 0 & 0 \end{bmatrix} \boldsymbol{T}_{H2}(\theta_{h2})\boldsymbol{T}_{P2}(\theta_{p2})\boldsymbol{T}_{P1}(\theta_{p1})\boldsymbol{T}_{H1}(\theta_{h1}) \begin{bmatrix} 1 & 0 \\ 0 & 0 \end{bmatrix}$$

$$\boldsymbol{T}_{\mathrm{CCW}} = \begin{bmatrix} 0 & 0 \\ 0 & 1 \end{bmatrix} \boldsymbol{T}_{H1}(-\theta_{h1})\boldsymbol{T}_{P1}(-\theta_{p1})\boldsymbol{T}_{P2}(-\theta_{p2})\boldsymbol{T}_{H2}(-\theta_{h2}) \times \begin{bmatrix} 0 & 0 \\ 0 & 1 \end{bmatrix}$$

Here, $\boldsymbol{T}_{H1}$, $\boldsymbol{T}_{H2}$, $\boldsymbol{T}_{P1}$ and $\boldsymbol{T}_{P2}$ are Jones transfer matrices of HWP 1, HWP 2, PMF 1 and PMF 2 that have orientation angles of θ_{h1}, θ_{h2}, θ_{p1} and θ_{p2}, respectively. $\theta_{p2} = \theta_{p1} + 60°$ because the two PMF loops are spliced with an offset angle of 60°. This angle offset gives the filter the capability of flat-top band and interleaving operation. The filter transmittance t can be derived from the transfer matrix $\boldsymbol{T}$ and is given by the following equation:

$$\begin{aligned} t = {} & \cos^2\left(\frac{\Gamma}{2}\right)\left\{\cos^2\Gamma\cos^2(2\theta_{h1} - 2\theta_{h2}) \right. \\ & \left. + \sin^2\Gamma\cos^2(2\theta_{h1} + 2\theta_{h2} - 2\theta_{p2})\right\} \\ & + \sin^2\left(\frac{\Gamma}{2}\right)\left\{\cos^2\Gamma\cos^2(2\theta_{h1} + 2\theta_{h2} - 2\theta_{p1}) \right. \\ & \left. + \sin^2\Gamma\cos^2(2\theta_{h1} - 2\theta_{h2} - 2\theta_{p1} + 2\theta_{p2})\right\} \\ & - cos\Gamma\sin^2\Gamma\sin(4\theta_{h1} - 2\theta_{p1})\sin(4\theta_{h2} - 2\theta_{p2}) \end{aligned} \tag{2}$$

where $\Gamma(=2\pi BL/\lambda)$ is a phase retardation difference between two orthogonally polarised modes along the principal axes of the PMF. It is generated because of birefringence B and length L of PMF 1 (λ is the wavelength in vacuum). The phase retardation difference of the HWPs was assumed to be independent of wavelength, and any insertion losses of optical components were not considered in the derivation of the filter transmittance.

From the filter transmittance in (2), various ideal (calculated) transmission spectra can be obtained by changing the orientation angles (θ_{h1}, θ_{h2}) of the two HWPs (HWP 1 and HWP 2). At the specific (θ_{h1}, θ_{h2}) combination given by Table 1, the proposed filter provides four specific transmission functions including flat-top and lossy flat-top band transmission spectra and their interleaved spectra. An interleaved spectrum signifies a spectrally shifted version of the original spectrum, of which switching displacement is half a channel spacing (or an interference period). t_{f}, $t_{f,i}$, t_{lf} and $t_{lf,i}$, shown in (3)–(6), indicate the transmittances of the proposed filter at these four specific transmission modes such as flat-top, interleaved flat-top, lossy flat-top and interleaved lossy flat-top band modes, respectively:

$$t_f = -\frac{1}{4}\cos^3\Gamma + \frac{3}{4}\cos\Gamma + \frac{1}{2} \tag{3}$$

$$t_{f,i} = \frac{1}{4}\cos^3\Gamma - \frac{3}{4}\cos\Gamma + \frac{1}{2} \tag{4}$$

$$t_{lf} = \alpha\cos^3\Gamma + \beta\cos^2\Gamma + \gamma\cos\Gamma + \delta \tag{5}$$

$$t_{lf,i} = -\alpha\cos^3\Gamma - \beta\cos^2\Gamma - \gamma\cos\Gamma + \delta \tag{6}$$

$$\left(\alpha = \frac{3}{8} + \frac{3}{4}\cos\frac{14}{51}\pi, \quad \beta = -\frac{3}{8} + \frac{\sqrt{3}}{4}\sin\frac{14}{51}\pi \right.$$
$$\left. \gamma = \frac{3}{8} + \frac{1}{4}\cos\frac{10}{51}\pi - \frac{1}{2}\cos\frac{7}{51}\pi, \quad \delta = \frac{5}{8} - \frac{1}{4}\cos\frac{10}{51}\pi\right)$$

As can be found from Table 1 and (3)–(6), the proposed filter is able to operate in a flat-top or a lossy flat-top band mode and be interleaved in each mode by proper selection of the orientation angles (θ_{h1}, θ_{h2}) of the two HWPs. Here, θ_{h1} and θ_{h2} have an angle symmetry of $\pi/2$ in (2) because of the intrinsic orientation angle symmetry of π in the HWP. Figs. 2*a* and *b* show the theoretically

Table 1 Four specific flat-top band transmission modes of the proposed filter

Transmission modes	θ_{h1}	θ_{h2}
flat-top band mode (t_f)	$(\theta_{p1} + \pi/4)/2$	$(\theta_{p1} + \pi/4)/2$
interleaved flat-top band mode ($t_{f,i}$)	$(\theta_{p1} - \pi/4)/2$	
lossy flat-top band mode (t_{lf})	$(\theta_{p1} + 2\pi/17)/2$	$(\theta_{p1} - 2\pi/17)/2 + \pi/4$
interleaved lossy flat-top band mode ($t_{lf,i}$)	$(\theta_{p1} - 2\pi/17)/2$	

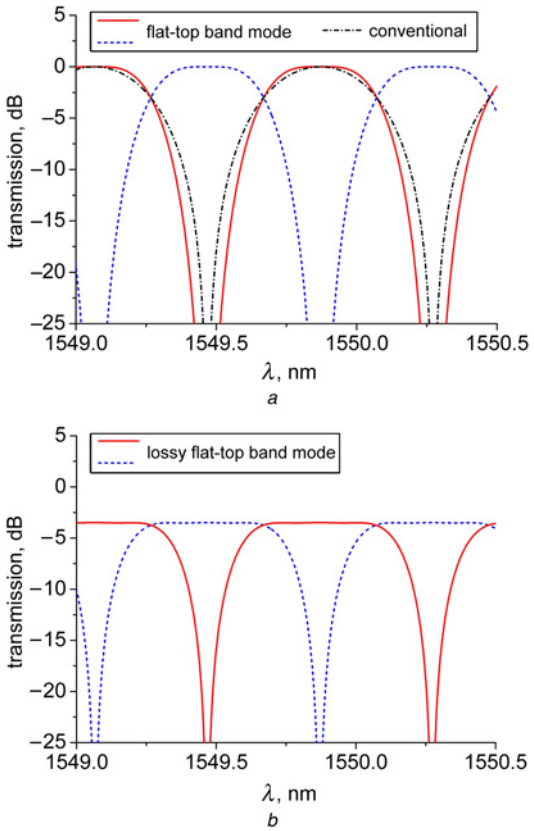

Figure 2 *Theoretically calculated transmission spectra*
a Flat-top band mode
b Lossy flat-top band mode

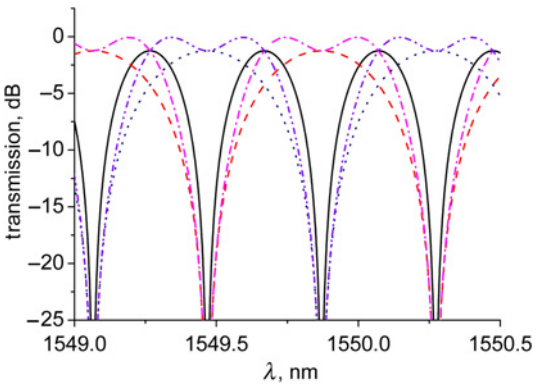

Figure 3 *Theoretically calculated transmission spectra for three non-optimal categories*

calculated ideal transmission spectra of the proposed filter, which are plotted with filter transmittances in flat-top and lossy flat-top band modes, given by (3) and (5), respectively. In the theoretical visualisation shown in Fig. 2, the PMF birefringence was set as 4.8×10^{-4} and the length of PMF 1 was set as 6.25 m so that the wavelength spacing between passband (channel) centres in the transmission spectrum could be 0.8 nm at 1550 nm for further comparison with measured spectra.

In Fig. 2, dashed curves are the interleaved versions of solid curves, and the transmission spectrum of the conventional Sagnac birefringence filter was added for comparison as a dashed–dotted curve. As can be seen from the Figure, the flat-top or lossy flat-top transmission spectrum can be interleaved by adjusting (θ_{h1}, θ_{h2}) of the two HWPs, which cannot be implemented in the previous Lyot-Sagnac high-order multiwavelength filter. For general combinations at other combinations of HWP angles, the filter has spectral characteristics like those shown in Fig. 3 [(solid line: category 1), (dashed and dotted lines: category 2) and (dashed–dotted and dash-double–dotted lines: category 3)]. The three categories are as follows: (i) a conventional (zeroth-order) Sagnac birefringence filter (SBF) with a channel spacing of 0.4 nm except an inherent insertion loss of 1.25 dB; (ii) a conventional (zeroth-order) SBF with a channel spacing of 0.8 nm except an inherent insertion loss of 1.25 dB; and (iii) a second-order flat-top passband filter with a channel spacing of 0.8 nm except a deteriorated band flatness and insertion loss. Moreover, categories 2 and 3 have interleaving capability. The specific HWP angle combinations for three non-optimal categories and corresponding filter transmittances are shown in Table 2. These general cases were also confirmed from the experiments. Moreover, compared with a Solc-type high-order multiwavelength filter, the proposed filter shows narrower passbands. Two figures of merit (FOM), indicated as −1 and −3 dB FOMs, were defined as −1 and −3 dB bandwidths of the proposed filter divided by the channel spacing for the quantitative comparison of the channel bandwidth, respectively. The channel spacing was 0.8 nm in the calculation of theoretical FOMs. As shown in Table 3, the theoretical −3 dB FOM was

Table 2 HWP angle combinations for three non-optimal categories and corresponding transmittances

	θ_{h1}	θ_{h2}	Transmittance
category 1	$\theta_{p1}/2$	$\theta_{p1}/2+\pi/4$	$(3/4)(1-\cos^2\Gamma)$
category 2	$(\theta_{p1}+\pi/6)/2$	$(\theta_{p1}+\pi/3)/2$	$(3/8)\cos\Gamma+(3/8)$
category 2 (interleaved)	$(\theta_{p1}-\pi/6)/2$		$-(3/8)\cos\Gamma+(3/8)$
category 3	$(\theta_{p1}+\pi/3)/2$	$(\theta_{p1}-\pi/6)/2$	$-(3/8)(\cos\Gamma+1)(\cos^2\Gamma-2)$
category 3 (interleaved)	$((\theta_{p1}-\pi/3)/2)$		$(3/8)(\cos\Gamma-1)(\cos^2\Gamma-2)$

Table 3 Comparison between theoretical and experimental FOMs

	Theoretical FOMs		Experimental FOMs	
	−1 dB FOM, %	−3 dB FOM, %	−1 dB FOM, %	−3 dB FOM, %
conventional zeroth-order filter	30	50	–	–
Solc-type first-order filter	~47.1	~63.6	–	–
proposed Lyot-type filter (flat-top band mode)	~36.4	50	~39	~52.7
proposed Lyot-type filter (lossy flat-top band mode)	~61	~73.2	~62.8	~75

evaluated as 50%, that is equal to that of the conventional filter, but the theoretical −1 dB FOM was evaluated as ~36.4%, which was greater than that of the conventional one, implying a flattened passband. Theoretical −1 and −3 dB FOMs were more than 10% smaller than those of the previous Solc-type high-order multiwavelength filter. This indicates that the proposed filter provides narrower passbands than a Solc-type high-order multiwavelength filter with the same order.

3. Experimental results and discussion: The four specific transmission modes mentioned above were experimentally investigated. To verify the theoretical results, the proposed filter was fabricated as shown in Fig. 1. The length of PMF 2 was tailored to be double in comparison with that of PMF 1, and PMF 1 and PMF 2 were concatenated with a 60° angle offset between their principal axes. Splicing points between two bowtie-type PMFs are marked with diamond symbols in Fig. 1. The PMF birefringence was $\sim 4.59 \times 10^{-4}$, and the lengths of PMF 1 and PMF 2 were ~6.25 and ~12.50 m, respectively, which were tailored for the channel spacing to be ~0.8 nm near 1550 nm. Figs. 4*a* and *b* show the measured transmission spectra of the fabricated filter in flat-top and lossy flat-top band modes, respectively. Like Fig. 2, dashed curves are interleaved versions of solid curves in both flat-top band modes shown in the Figure. A flat-top and a lossy flat-top band mode were obtained at (θ_{h1}, θ_{h2}) = (126°, 234°) and (126°, 280°), and their interleaved versions at (θ_{h1}, θ_{h2}) = (26°, 49°) and (4°, 49°), respectively. In both modes, the switching displacement between the two transmission curves, that is, solid and dashed curves, was measured as ~0.4 nm. It is confirmed from these experimental results that the proposed filter can operate in a flat-top band mode or a lossy flat-top band mode, and the multiwavelength filter channel can be interleaved in those modes through the orientation angle adjustment of the two HWPs. It is observed in Fig. 4 that the spectral shape of the measured transmission spectra is very similar to that of the theoretically predicted ones, except for the decreased extinction ratio and the increased insertion loss. The insertion losses were measured as ~3.8 dB and ~6.5 dB in the flat-top and the lossy flat-top band modes, respectively. The extinction ratios were measured as >22.8 dB and >14.2 dB in the flat-top and lossy flat-top band modes, respectively. At other wavelength bands beyond the spectral range shown in Fig. 4, the extinction ratio of the proposed filter continues to decrease with the increase of the wavelength deviation from 1550 nm and is reduced down to 20 dB at a wavelength of 1547 nm or 1553 nm. Deterioration of the insertion losses and the extinction ratios can be caused by the wavelength dependency of the HWPs, tailoring errors of the PMF length and the weak inherent birefringence of the single-mode fibre used to connect optical components comprising the proposed filter [20].

To make a quantitative comparison between the passband bandwidths of the proposed filter and other filters, both −1 and −3 dB

doi: 10.1049/mnl.2014.0386

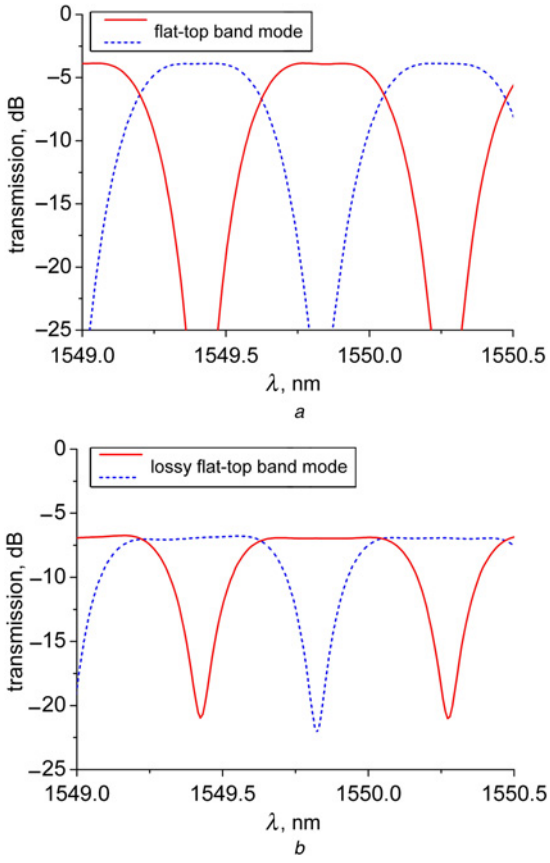

Figure 4 *Experimentally measured transmission spectra*
a Flat-top band mode
b Lossy flat-top band mode

passband bandwidths of a conventional zeroth-order filter, a Solc-type first-order filter and the proposed filter (including the flat-top and the lossy flat-top band modes) were considered and compared with each other. Experimental −1 and −3 dB FOMs of the proposed filter were evaluated using the measured −1 and −3 dB bandwidths of the proposed filter. As shown in Table 3, the experimental −1 and −3 dB FOMs were evaluated as ∼39 and ∼52.7% in the flat-top band mode and as ∼62.8 and ∼75% in the lossy flat-top band mode, respectively. The difference between theoretical and experimental FOMs is within 2.6%. This FOM deviation is expected to result from inherent birefringence of the single-mode fibre and the tailoring error of the PMF. In particular, although the lossy flat-top band mode is accompanied by the inherent insertion loss of ∼3.49 dB, its theoretical −3 dB FOM increases up to ∼73.2%, and its −1 dB FOM is improved more than twice in comparison with that of the conventional zeroth-order filter. The lossy flat-top band mode provides a bandwidth performance close to the flat-top band mode of the Solc-type second-order filter that employs three PMF loops. In addition, in the flat-top band mode of the proposed filter, −1 and −3 dB FOMs are smaller by 10.7 and 13.6% than those of the Solc-type first-order filter, respectively. The narrower passband of the proposed filter can be beneficially utilised in reducing unwanted channel noises at spectral locations deviated from a passband centre.

4. Conclusion: The Lyot-type flat-top fibre multiwavelength filter was demonstrated by incorporating the PDLS. The proposed filter has polarisation-independent flat-top passbands and multiwavelength switching capability. The high-order transmission function was realised by concatenating two PMF loops with different lengths in the PDLS according to the Lyot-type arrangement of birefringence elements. By controlling the two HWPs, high-order transmission spectra such as the flat-top and the lossy flat-top transmission spectra could be obtained, and flat-top passbands could be also interleaved in both modes, which could not be obtained in the previous Lyot-Sagnac comb filter based on a fibre coupler. Experimental −1 and −3 dB FOMs for bandwidth comparison were evaluated as ∼39 and ∼52.7% in the flat-top band mode and ∼62.8 and ∼75% in the lossy flat-top band mode, respectively. In particular, the proposed filter provides narrower passbands, compared with a Solc-type first-order multiwavelength filter.

5. Acknowledgments: This work was supported by the Power Generation and Electricity Delivery Core Technology Program of the Korea Institute of Energy Technology Evaluation and Planning (KETEP) that granted financial resources from the Ministry of Trade, Industry and Energy, Republic of Korea (no. 20131020400830).

6 References

[1] Hasegawa T., Inoue K., Oda K.: 'Polarization independent frequency conversion by fiber four-wave mixing with a polarization-diversity technique', *IEEE Photonics Technol. Lett.*, 1993, **5**, pp. 947–949
[2] Lee Y.W.: 'Polarization-independent multiwavelength-switchable filter based on polarization beam splitter and fiber coupler', *KIEE J. Electr. Eng. Technol.*, 2009, **4**, pp. 405–409
[3] Lee Y.W., Han K.J., Jung J., Lee B.: 'Polarization-independent tunable fiber comb filter', *IEEE Photonics Technol. Lett.*, 2004, **16**, pp. 2066–2068
[4] Lee Y.W., Han K.J., Lee B., Jung J.: 'Polarization-independent all-fiber multiwavelength-switchable filter based on a polarization-diversity loop configuration', *Opt. Express*, 2003, **11**, pp. 3359–3364
[5] Zhu G., Wang Q., Chen H., Dong H., Dutta N.K.: 'High-quality optical pulse train generation at 80 Gb/s using a modified regenerative-type mode-locked fiber laser', *IEEE J. Quantum Electron.*, 2004, **40**, pp. 721–725
[6] Fang X., Demarest K., Ji H., Allen C., Pelz L.: 'A subnanosecond polarization-independent tunable filter/wavelength router using a Sagnac interferometer', *IEEE Photonics Technol. Lett.*, 1997, **9**, pp. 1490–1492
[7] Rossi G., Jerphagnon O., Olsson B., Blumenthal D.J.: 'Optical SCM data extraction using a fiber-loop mirror for WDM network systems', *IEEE Photonics Technol. Lett.*, 2000, **12**, pp. 897–899
[8] Yoon I., Lee Y.W., Jung J., Lee B.: 'Tunable multiwavelength fiber laser employing a comb filter based on a polarization-diversity loop configuration', *J. Lightwave Technol.*, 2006, **12**, pp. 1805–1811
[9] Kim C.S., Kang J.U.: 'Multiwavelength switching of Raman fiber ring laser incorporating composite polarization-maintaining fiber Lyot-Sagnac filter', *Appl. Opt.*, 2004, **43**, pp. 3151–3157
[10] Lee Y.W., Jung J., Lee B.: 'Multiwavelength-switchable SOA-fiber ring laser based on polarization-maintaining fiber loop mirror and polarization beam splitter', *IEEE Photonics Technol. Lett.*, 2004, **16**, pp. 54–56
[11] Ryu C.-H., Jung S.-Y., Koo J.-Y., Yeon M.-S.: 'An application of the novel techniques detecting partial discharge employable to GIS using optical fiber', *KIEE J. Electr. Eng. Technol.*, 2007, **2**, pp. 396–400
[12] Ryu H.-S., Han G.-H., Yoon N.-S.: 'The method of determining stress levels regarding the electrical ALT through optical temperature sensor', *KIEE J. Electr. Eng. Technol.*, 2008, **3**, pp. 184–191
[13] Jung H., Kim J.-Y., Chang K.-T., Jung C.-S.: 'Slope movement detection using ubiquitous sensor network', *KIEE J. Electr. Eng. Technol.*, 2009, **4**, pp. 143–148
[14] Fang X., Claus R.O.: 'Polarization-independent all-fiber wavelength-division multiplexer based on a Sagnac interferometer', *Opt. Lett.*, 1995, **20**, pp. 2146–2148
[15] Lee Y.W., Kim H.-T., Jung J., Lee B.: 'Wavelength-switchable flat-top fiber comb filter based on a Solc type birefringence combination', *Opt. Express*, 2005, **13**, pp. 1039–1048
[16] Jia Z., Chen M., Xie S.: 'Label erasing technique employing Lyot-Sagnac filter', *Electron. Lett.*, 2002, **38**, pp. 1563–1564
[17] Özgören K., Ilday F.Ö.: 'All-fiber all-normal dispersion laser with a fiber-based Lyot filter', *Opt. Lett.*, 2010, **35**, pp. 1296–1298
[18] Yan Z., Mou C., Wang H., *ET AL.*: 'All-fiber polarization interference filters based on 45°-tilted fiber gratings', *Opt. Lett.*, 2012, **37**, pp. 353–355
[19] Solc I.: 'Birefringent chain filters', *J. Opt. Soc. Am.*, 1965, **55**, pp. 621–625
[20] Kim Y., Lee Y.W.: 'Study on spectral deviations of high-order optical fiber comb filter based on polarization-diversity loop configuration', *Opt. Commun.*, 2013, **301–302**, pp. 159–163